Dalton Transactions

Accepted Manuscript

ROYAL SOCIETY OF CHEMISTRY

www.rsc.org/dalton

Journal Name

ARTICLE

Highly selective fluorescence sensors for the fluoride anion based on carboxylate-bridged diiron complexes

Received 00th January 20xx,
Accepted 00th January 20xx

DOI: 10.1039/x0xx00000x

www.rsc.org/

Yuhan Zhou*, Xiaoliang Dong, Yixin Zhang, Peng Tong, and Jingping Qu*

ABSTRACT: A new ligand bearing anthracene and its Fe(III) and Ru(III) derivatives have been synthesized and characterized exactly. The studies show that these dinuclear metal complexes serve as candidates of fluorescence chemosensors for anions. The interactions between these complexes and anions have been investigated by means of UV-Vis absorption spectra, fluorescence spectra, titration studies and ^{1}H-NMR. The results illustrated that two diiron complexes, [Cp*Fe(μ-SR)$_2$(μ-η^2-L)FeCp*][PF_6] (**5a**, R = Me; **5b**, R = Et; L = 4-(3-(anthracen-9-ylmethyl)ureido)benzoate), showed rapid and selective recognition for fluoride ion over other anions with strong enhancement of emission intensities. The sensing mechanisms indicate that the hydrogen bonding interaction has been observed between chemosensors and F^-.

Introduction

The recognition and sensing of anions has been a key research theme within the generalized area of supramolecular chemistry because of the important role of anions in biological and environmental fields.[1,2] Particularly, of the different biological anions, fluoride is of special interest owing to its role in preventing dental caries[3] and in the treatment for osteoporosis.[4] Apart from their essential roles, excess fluoride can cause dental or skeletal fluorosis,[5] and it is also associated with kidney failure[6] and nephrolithiasis.[7] Thus, the development of reliable sensing methods for fluoride is urgently desired because of diversity of their functions.

Recently, metal complexes derived sensors have been studied, mainly due to the sensitivity of emission properties and relatively long lifetime compared with purely organic chemosensors. Among them, ruthenium based chemosensors have been well developed for sensing fluoride ions.[8] The other metal complexes, such as Re(I)[8i], Co(II),[8f,9] Al(III),[10] Zn(II),[11] Zr(II),[12] Pt(II),[13] Eu(III),[14] *etc*. have also been documented. To the best of our knowledge, few examples of the chemosensor bearing iron metal for the detection of fluoride anion have been reported and most of these compounds derived from ferrocene.[15] But, the deficiencies of the reported iron compounds are as follows: (1) The selectivity for fluoride anion is not very good.[15a] (2) Parts of compounds need to use electrochemical analyser to detect fluoride anion, which is inconvenient and non-real-time.[15c,d]

Recently, our group aims at the synthesis and reactivity of diiron-sulfur clusters with Cp* as ancillary ligands, which can provide bimetallic reaction sites and simulate biological metalloproteins. The reactivity of these diiron-sulfur clusters with some small molecules, such as hydrazines, alkynes, CS_2, alcohol/aldehyde and carboxylate salts have been well explored.[16] Some metalloenzymes, such as Ribonucleotide reductase (RNR)[17] and soluble methane monooxygenase (sMMO),[18] contain carboxylate-bridged diiron cores and F^- perform a variety of functions in biological systems,[19] which inspire us to model the core of these enymes for detecting F^-. In this context, we present the formation of carboxylate-bridged cyclopentadienyl diiron and diruthenium bearing urea and anthracene units. Importantly, the two diiron-sulfur clusters behave as highly selective chemosensors for fluoride ion over other anions. This reveals the important application of diiron-sulfur clusters in chemosensors.

Results and discussion

Synthesis and characterization

The synthetic procedure for chemosensors **5** [Cp*M(μ-SR)$_2$(μ-η^2-L)MCp*][PF_6] (**5a**, M = Fe, R = Me; **5b**, M = Fe, R = Et; **5c**, M = Ru, R = Et; L = 4-(3-(anthracen-9-ylmethyl)ureido)benzoate) is shown in scheme 1. Compound **3** was obtained by the addition reaction of **1** with **2** and then hydrolysis in 52% yield. The reactions of potassium carboxylate (prepared by the reaction of **3** with *t*-BuOK) with complexes **4** were carried out to give complexes **5** in moderate yield. These new compounds were characterized by ^{1}H-NMR and HRMS and the complexes **5a** - **5c** were further characterized by IR spectroscopy and X-ray diffraction

The ^{1}H NMR spectrum of **5a** in CD_2Cl_2 exhibits some resonances at δ 6.72, 5.25, 1.79 and 1.43 ppm corresponding to NH, CH_2, CH_3 and Cp*. What's more, the peak at δ 5.33 for CH_2 and the signal of the other NH of urea group overlay with the sovlent's (CD_2Cl_2). For **5b**, the resonances at δ 6.73 and 5.26 were attributed to two NH. It

State Key Laboratory of Fine Chemicals, School of Pharmaceutical Science and Technology, Dalian University of Technology, Dalian, 116024, P.R. China
Email: zhouyh@dl.cn (Y.Z.);
Email: qujp@dlut.edu.cn (J.Q.).
Electronic Supplementary Information (ESI) available: Experiment section, spectra and Crystal structures. CCDC reference numbers 1415233-1415235. X-ray crystallographic data in CIF format. See DOI: 10.1039/x0xx00000x

should be noted that the chemical shift of two equivalent CH_3 (1.92, ppm, triplet) of -SEt group was higher than that of two equivalent CH_2 (1.63 ppm, quartet) of -SEt group. This abnormal result is caused by shielding effect of Fe1-Fe2-O2-C25-O1 cycle, which is fully consistent with the X-ray structure of **5b**. But, unlike **5b**, the abnormal results in the ^{1}H NMR spectra of **5c** were not observed even if their structures were similar to each other. Complex **5c** exhibits resonances at δ 2.03 and 1.47 ascribed to CH_2 and CH_3 of –SEt respectively.

Crystal structures

The structures of **5a**, **5b** and **5c** are unambiguously characterized by single crystal X-ray diffraction analysis, and their spectral features are fully consistent with their crystal structures. Their crystallographic data are listed in Table 1 and their ORTEP drawings and selected bond distances and angles are shown in Fig. 1 to Fig. 3.

Fig. 1 to Fig. 3

Table 1

These three complexes have similar structures. The two M(III) (M = Fe and Ru) centers are bridged by a μ-1,3 carboxylate ligand and two –SR (R = Me or Et) ligands. In complex **5a**, the distance of Fe–Fe 2.5996(10) Å falls in the 2.5-2.8 Å range which indicates a single bond between the two iron atoms.[20] The two Cp* ligands coordinating to Fe centers are in mutually *cis*- orientation with dihedral angle being 55.94(15)°. The distance of Fe-S and Fe-O is approximate 2.21 Å and 1.97 Å. Similar to **5a**, the distance of Fe–Fe 2.6208(8) Å in **5b** falls in the 2.5-2.8 Å range. The Fe2S2 ring is substantially puckered with a dihedral angle of 172.64(6)° along the Fe(1)–Fe(2) vector. The distances of Fe–O are 1.972(3) Å and 1.976(3) Å, being agreement with that observed in the analogous structure of **5a**. The angle of O(1)–C(25)–O(2) is 124.8(3)°. The dihedral angle between $\{Fe_2(\mu\text{-}O_2)\}^{2+}$ plane and O(1)–C(25)–O(2) plane being 1.2(4)° indicates they are almost on the same plane. From the structure of **5b**, we can also see that the two equivalents CH_2 of -SEt locate in the chemical shielding zone of Fe(1)-Fe(2)-O(2)-C(25)-O(1) cycle, which makes CH_2 of -SEt shift to up-field in ^{1}H NMR spectrum.

For **5c**, the distance of Ru-Ru is 2.7080(4), which shows a single bond between the two Ru atoms. Notably, The dihedral angle of complex **5c** between $\{Ru_2(\mu\text{-}O_2)\}^{2+}$ plane and O(1)–C(25)–O(2) plane is 5.9(2)°, which is larger than that in **5a** and **5b** (4.4(4)° and 1.2(4) respectively).

UV-Vis absorption

Initially, the UV-Vis absorption of **5a** to **5c** towards F^- ion and other anions were studied in THF solution. As shown in Fig. 4 and Fig. S1 (ESI), **5a** and **5b** exhibit typical anthracene absorption bands at 345, 367 and 385 nm respectively (ε = 34500, 29600, 26000 and 16200, 16000, 13600 $M^{-1}\cdot cm^{-1}$). There are slight changes upon addition of 3 equiv of various anions to the THF solution of **5a** or **5b**. UV-Vis absorption titrations of **5a** in the presence of different equivalents of F^- were performed. As shown in Fig S2 (ESI), F^- have little impact on the intensity of the absorption **5a**. Similar to **5a** or **5b**, no significant response of **5c** was observed upon addition of various anions, as illustrated in Fig S3 (ESI).

Fig. 4

Fluorescence study

Despite the presence of anthracene fluorophore unit of chemosensor **5a** and **5b**, the fluorescent emission intensity of **5a** and **5b** were much lower than Ligand **3**, as shown in Fig. 5. It resulted from quenching process through photo-induced electron transfer mechanism (PET mechanism)[21] and the heavy atoms effect. However, as shown in Fig. 6, a solution of **5a** in THF (1×10^{-5} M) showed strong fluorescence emission upon addition of F^- ion (as its TBA salt) excited with 370 nm (slit width = 3 nm) and the emission intensity gradually increased with the continual addition of F^- (0 - 3 equiv). It was different from the Santos work,[2g] which showed the decreasing in fluorescent emission intensity upon addition of F^-. The opposite results might be attributed to the effect of diiron center. A good linear relationship between the ratio of I/I_0 and the fluoride ion concentration was obtained (R^2 = 0.97221) as depicted in the inset in Fig. 6, which indicated chemosensor **5a** was a good ratiometric sensor for F^- ion. According to the general method for calculating the detection limit,[22] the F^- concentration at I/I_0 (the signal to background ration) = 3 is 9 μM, which is much lower than the enforceable drinking water standard for fluoride of 221 μM (4 mg/L) given by the EPA (United States Environmental Protection Agency). This showed that chemosensor **5a** had sufficient high sensitivity to detect F^- even at low concentration by fluorescence spectrophotometer.

Fig. 5 and Fig. 6

In order to evaluate the selectivity of chemosensor **5a**, various anions including F^-, Br^-, Cl^-, HSO_4^-, CH_3COO^-, NO_3^-, I^- and $H_2PO_4^-$ were incubated individually with chemosensor **5a** in THF. From the Fig. 7, it can be seen that the fluorescence intensity of chemosensor **5a** markedly increased upon the addition of F^- ion, which may be ascribed to strong hydrogen bonding interaction between F^- ion and the NH unit of urea group because of high charge density and small size of F^- ion,[23] whereas all the other anions examined caused negligible changes. This result meant that chemosensor **5a** showed high selectivity for F^- over other anions. As far as we know, this is the first example of chemosensor for F^- based on the diiron complex.

Fig. 7

To determine the binding stoichiometry between chemosensor **5a** and F^- ion, Job's method was employed with the changes of fluorescent emission at 414 nm as a function of molar fraction of F^-.[23] It exhibited a maximum emission at a mole fraction of 0.5 (Fig. 8), indicating that the complex stoichiometry of F^- was 1:1 for **5a**.

Fig. 8

Similar to **5a**, the fluorescent emission of chemosensor **5b** were greatly affected by F^- ion. The fluorescence of **5b** was gradually turned on with stepwise addition of F^- ion, as shown in Fig. 9. From the inset of Fig. 9, it could be also concluded that the detection limit of **5b** for F^- is 6.7 μM, lower than 9 μM of chemosensor **5a**. Upon addition of other anions such as Br^-, Cl^-, HSO_4^-, CH_3COO^-, NO_3^-, I^- and $H_2PO_4^-$, no detectable changes were observed, as illustrated in Fig. 10. We learnt that many other chemosensors based on ferrocene had poor selectivity for F^-, which were interfered by AcO^-, DBU and so on.[15c,d,f] The fluorescence of some of chemosensors was quenched by F^-, which was different from **5a** and **5b**. The high binding affinity and efficient fluorescence enhancement by F^- over

other anions probably resulted from F^- ion being a strong hydrogen bonding acceptor that shows interaction with NH unit of urea group.[24] According to the job's plot illustrated in Fig. S4 (ESI), it could be concluded that the complex stoichiometry of F^- was 1:1 for **5b**.

Fig. 9 and Fig. 10

For establishing the effects of coexisting relevant anions on the detection of F^-, the experiments with the possible interferents together with F^- have been done, as illustrated in Fig S5 (ESI). It can be seen that Ac^-, HSO_4^- and I^- have serious effects on the emission intensity of chemosensor **5b** in the presence of F^-. The slight interference have been found between F^- and Cl^-, NO_3^- or $H_2PO_4^-$. The possible reasons are that the hydrogen bond between the interfering anions (Ac^-, HSO_4^-, NO_3^- or $H_2PO_4^-$) and **5b** might also be formed and then compete with that of F^-. Because of heavy atom effect, I^- make the emission intensity decrease in the system of F^- and **5b**. However, emission intensity almost keeps unchanged before and after adding Br^- to a solution of **5b** and F^-. So, it can be concluded that Ac^-, HSO_4^- and I^- give remarkably interfered results and NO_3^-, $H_2PO_4^-$ and Cl^- give slightly interfered results. Br^- has an ignored effect on the intensity of **5b** in the presence of F^-.

In order to show the difference of fluorescent emission intensity between ligand **3** and complexes **5a** or **5b** in the presence of F^-, the plots were made, as shown in Fig. 5. It could be found that the fluorescent emission intensity of complexes **5a** or **5b** in the presence of F^- is lower than that of **3**. It is also observed that the fluorescence **5a** or **5b** undergoes a slight blue-shift. The results show that the diiron have an obviously effect on the fluorescence of ligand **3**.

Subsequently, the carboxylate-bridged diruthenium **5c** with Cp* and -SEt as ligands, structural similarity to **5b**, was also studied towards various anions in fluorescent emission changes. Unfortunately, as shown in Fig. S6 (ESI), there are no obvious changes towards F^- ion or other anions. The reason for this phenomenon is that the heavy atom Ru seriously quench the fluorescence.[25]

^{1}H NMR study and ESI-HRMS

To the chemosensor **5b**, further investigation of the insights into the nature of recognition for F^- anion was carried out by the analysis of ^{1}H NMR spectra. Considering the solubility of **5b** and TBAF, CD_3CN was chosen as solvent. The signals at δ 7.04 ppm and 5.56 ppm were ascribed to the NH of urea because they were not observed upon addition of D_2O to the solution of **5b** in CD_3CN, as illustrated in Fig. S7 (ESI). These two protons signal also entirely disappeared when adding 1 equivalent of F^- (as its TBA salt in CD_3CN) to CD_3CN solution of chemosensor **5b**, as shown in Fig. 11a and Fig. 11b, which indicated the formation of strong hydrogen bonding interactions between F^- and N-*H*.[26] As depicted in Fig. 11c to Fig. 11e, however, No changes were observed upon addition of more F^- (2 to 4 equivalent). It implied that the complex stoichiometry of F^- was 1:1 for **5b**, which was consistent with **5a**. From the inset of Fig.11, it should be noted that the number of peaks of aromatic and anthracene ring's proton signals decreased and their proton signals shift slightly after adding the F^- ion into the solution, but the number of H kept unchanged, which showed that hydrogen-bonding interaction between urea subunit and F^- ion could induce some effects on aromatic protons.

Fig. 11

To confirm the stability of complex **5b** in the presence of F^-, ESI-HRMS was proceeded, as shown in Fig. S8 (ESI). It can be seen that m/z = 873.2510 was found after adding 2 equivalent of F^- into the THF solution of **5b**, which corresponded to the calculated value of 873.2509 for $[\mathbf{5b}\text{-}PF_6]^+$. Thus, we could conclude that complex **5b** was stability in the presence of F^-.

Conclusions

We have designed and synthesized three carboxylate-bridged diiron and diruthenium sulfur complexes with anthracene as fluorophore and urea as binding site. The two diiron complexes show highly selective recognition for F^- ion over other anions through the hydrogen bonding interaction with urea and the detection limit for F^- ion is much lower than drinking water standard given by EPA. This is the first example of chemosensor for F^- based on the diiron complex.

Experiment

THF, CH_3CN, CH_2Cl_2, Hexane and Et_2O were distilled under argon before they were used. Infrared spectra were recorded on a NEXUSTM FT-IR spectrometer. The ^{1}H NMR spectra were performed on a Bruker 400 Ultra Shield spectrometer. The MS were measured on a LTQ Orbitrap XL TM spectrometer. Element analyses were performed on a Vario EL analyser. UV-Vis spectra were obtained on an HP 8453 spectrometer. Fluorescence spectra were obtained on a JASCO FP-6500 spectrofluometer with a 1 cm standard quartz cell. X-ray crystallography. Crystals suitable for X-ray crystallography were obtained by recrystallization from a mixture of Et_2O and CH_2Cl_2 or Hexane and CH_2Cl_2. The data were obtained on a Bruker SMART APEX CCD diffractometer with graphite-monochromated Mo Kα radiation (λ = 0.71073 Å). Empirical absorption corrections were performed using the SADABS[27] program. Structures were solved by direct methods and refined by full-matrix least-squares based on all data using F^2 using Shelx97.[28] All of the non-hydrogen atoms were refined anisotropically. All of the hydrogen atoms were generated and refined in ideal positions. Compound $[Cp^*Fe(\mu\text{-}SEt)_2(MeCN)_2FeCp^*][PF_6]_2$ (**4b**) was prepared according to our previous work.[16c] Compound **4a** was synthesized when MeSSMe took the place of EtSSEt according to the synthetic procedure of **4b**. The synthetic procedure of compound **4c** was shown in ESI.

Synthesis of 4-(3-(anthracen-9-ylmethyl)ureido)benzoic acid (3)

To a solution of anthracen-9-ylmethanamine (**1**, 1 g, 4.8 mmol) in CH_2Cl_2 (180 mL) was added methyl 4-isocyanatobenzoate (**2**, 0.86 g, 4.8 mmol) and then the resulting solution was stirred at room temperature for 24 h. The mixture was filtered and washed with $CHCl_3$ to give the yellow solid. To a solution of yellow solid in EtOH (15 mL) was added NaOH solution (2 M, 15 mL) and the resulting solution was stirred at 75 ^{o}C for 12 h. After being adjusted to pH = 6 with diluted hydrochloric acid (3 M), the solution was filtered and washed with H_2O and EtOH to give yellow crude solid. The solid was crystallized from DMSO-acetone to give light yellow solid **3** (0.92 g, 52%). ^{1}H NMR (400 MHz, DMSO-D^6): δ 11.24 (br, 1H), 8.99 (s, 1H), 8.61 (br, 1H), 8.54 (d, $J_{H\text{-}H}$ = 8.0 Hz, 2H), 8.11 (br, 2H), 7.72 (br, 2H), 7.54-7.61 (m, 4H), 7.35 (br, 3H), 5.31 (br, 2H). ^{13}C NMR (100 MHz,

DMSO-D^6): δ 155.1, 141.5, 131.1, 130.9, 129.8, 128.8, 127.1, 126.2, 125.2, 124.6, 115.9, 35.2. ESI-HRMS (*m/z*): $[M-H]^-$ 369.1317; calcd. value for $C_{23}H_{18}N_2O_3$: 369.1326.

General procedures for preparation of 5a - 5c

The reaction of **3** (72 mg, 0.19mmol) with *t*-BuOK (22 mg, 0.19 mmol) was carried out in THF (30 mL) solution at 50 ^oC for 2 h. The solution was removed in *vacuum* to give the potassium carboxylate. To a solution of the potassium carboxylate was added **4** (0.17 mmol) in CH_3CN (30 mL) and then the resulting solution was allowed to react for 48 h at 25 ^oC under argon. After filtration, the solution was removed in *vacuum*. Then, the residue was extracted with CH_2Cl_2 (3 mL). After removal of the solvent in *vacuum*, the residue was extracted with THF (3 mL). After removal of the solvent, the residue was washed with Et_2O (2 mL × 2) to give light green solid **5**.

5a: light green solid (108 mg, 60%). ^1H NMR (400 MHz, CD_2Cl_2): δ 8.43 (s, 1H), 8.32 (br, 2H), 7.99 (br, 2H), 7.44-7.50 (m, 4H), 7.13 (br, 2H), 6.95 (br, 2H), 6.72 (s, 1H), 5.25 (br, 2H), 1.79 (s, 6H), 1.43 (s, 30H). IR (KBr, cm^{-1}): 3419 (m), 2921 (s), 1695 (m), 1597 (m), 1550 (m), 1516 (s), 1397 (s), 1375 (m), 1318 (w), 1216 (w), 1178 (m), 1018 (m), 955 (w), 842 (s), 778 (m), 735 (m). ESI-HRMS (*m/z*): $[M-PF_6]^+$ 845.2170; calcd. value for $C_{45}H_{53}Fe_2N_2O_3S_2$: 845.2196. Anal. Calcd for $C_{45}H_{53}F_6Fe_2N_2S_2O_3P{\cdot}1.5CH_2Cl_2$: C, 49.95; H, 5.05. Found: C, 49.83; H, 5.10.

5b light green solid (105 mg, 58%). ^1H NMR (400 MHz, CD_2Cl_2): δ 8.44 (s, 1H), 8.33 (d, J_{H-H} = 8.0 Hz, 2H), 8.01 (d, J_{H-H} = 8.0 Hz, 2H), 7.46-7.51 (m, 4H), 7.14 (d, J_{H-H} = 8.0 Hz, 2H), 6.93 (d, J_{H-H} = 8.0 Hz, 2H), 6.73 (s, 1H), 5.33 (br, 2H), 5.26 (br, 1H), 1.93 (t, J_{H-H} = 8.0 Hz, 6H), 1.63 (q, J_{H-H} = 8.0 Hz, 4H), 1.46 (s, 30H). IR (KBr, cm^{-1}): 3421 (m), 3056 (w), 2981 (m), 2925 (s), 1698 (s), 1597 (s), 1519 (s), 1448 (w) 1403 (s), 1375 (m), 1319 (m), 1231 (m), 1178 (m), 1073 (w), 1018 (s), 845 (s), 778 (m), 736 (m). ESI-HRMS (*m/z*): $[M-PF_6]^+$ 873.2506; calcd. value for $C_{47}H_{57}Fe_2N_2O_3S_2$: 873.2509. Anal. Calcd for $C_{47}H_{57}F_6Fe_2N_2S_2O_3P$: C, 55.41; H, 5.64. Found: C, 54.73; H, 5.42.

5c brown solid (30 mg, 33%) ^1H NMR (400 MHz, CD_2Cl_2): δ 8.46 (s, 1H), 8.36 (d, J_{H-H} = 8.0 Hz, 2H), 8.02 (d, J_{H-H} = 8.0 Hz, 2H), 7.46-7.55 (m, 6H), 7.31 (d, J_{H-H} = 8.0 Hz, 2H), 6.80 (s, 1H), 5.36 (d, J_{H-H} = 8.0 Hz, 2H), 5.29 (br, 1H), 2.03 (q, J_{H-H} = 8.0 Hz, 4H), 1.79 (s, 30H), 1.47 (t, J_{H-H} = 8.0 Hz, 6H). IR (KBr, cm^{-1}): 3423 (s), 3062 (w), 2972 (m), 2924 (m), 1698 (s), 1596 (s), 1538 (s), 1452 (w) 1396 (s), 1375 (m), 1317 (m), 1220 (m), 1178 (m), 1023 (s), 955 (w), 845 (s), 778 (m), 737 (m). ESI-HRMS (*m/z*): $[M-PF_6]^+$ 965.1911; calcd. value for $C_{47}H_{57}Ru_2N_2O_3S_2$: 965.1898. Anal. Calcd for $C_{47}H_{57}F_6Ru_2N_2S_2O_3P$: C, 50.89; H, 5.18. Found: C, 49.90; H, 4.86.

Acknowledgements

The authors gratefully acknowledge the financial support of the National Natural Science Foundation of China (No. 21376040, 21231003), Zhejiang Provincial Top Key Academic Discipline of Chemical Engineering and Technology, Zhejiang Sci-Tech University (No. YR2013012), and the program for Changjiang Scholars and Innovative Research Team in University (No. IRT13008). We also thank Prof. Baomin Wang, Dr. Ying Peng and Dr. Yuming Song for valuable discussions.

References

1 (a) J.-M. Lehn, Supramolecular Chemistry: Concepts and Perspective, VCH, Weinheim, 1995; (b) A. Bianchi, K. Bowman-James and E. García-Espana, Supramolecular Chemistry of Anions, Wiley-VCH Publishers, Toronto, Canada, 1997.

2 (a) P. A. Gale, N. Busschaert, C. J. E. Haynes, L. E. Karagiannidis and I. L. Kirby, *Chem. Soc. Rev.,* 2014, **43**, 205-241; (b) F. Wang, L. Wang, X. Chen and J. Yoon, *Chem. Soc. Rev*., 2014, **43**, 4312-4324; (c) X. Chen, Y. Zhou, X. Peng and J. Yoon, *Chem. Soc. Rev*., 2010, **39**, 2120-2135; (d) L. Fabbrizzi and A. Poggi, *Chem. Soc. Rev*., 2013, **42**, 1681-1699; (e) M. Cametti and K. Rissanen, *Chem. Soc. Rev*., 2013, **42**, 2016-2038. (f) V. B. Bregović, N. Basarić and K. Mlinarić-Majerski, *Coord. Chem. Rev.,* 2015, **295**, 80-124; (g) C. M. G. Dos Santos, M. Glynn, T. Mccabe, J. Sérgio Seixas de Melo, H. D. Burrows and T. Gunlaugsson, *Supramol. Chem*., 2008, **20**, 407-418.

3 K. L. Kirk, Biochemistry of Halogens and Inorganic Halides, Plenum, New York, 1991.

4 (a) M. Kleerekoper, *Endocrinol. Metab. Clin. North Am*. 1998, **27**, 441–452; (b) D. Briancon, *Rev. Rhum*. 1997, **64**, 78–81.

5 E. T. Everett, *J. Dent. Res*. 2011, **90**, 552–560.

6 (a) M.-L. Cittanova, B. Lelongt, M.-C. Verpont, M. Géniteau-Legendre, F. Wahbé, D. Prié, P. Coriat and P. M. Ronco, *Anesthesiology* 1996, **84**, 428–435; (b) M. Ludlow, G. Luxton and T. Mathew, *Nephrol. Dial. Transplant* 2007, **22**, 2763–2767.

7 P. P. Singh, M. K. Barjatiya, S. Dhing, R. Bhatnagar, S. Kothari and V. Dhar, *Urol. Res*. 2001, **29**, 238–244.

8 (a) S. J. Dickson, S. C. G. Biagini and J. W. Steed, *Chem. Commun*., 2007, 4955–4957; (b) A. Mishra, V. Vajpayee, H. Kim, M. H. Lee, H. Jung, P. J. Stang and K. W. Chi, *Dalton Trans*., 2012, **41**, 1195-1201; (c) J.-L. Fillaut, J. Andriès, L. Toupet and J.-P. Desvergne, *Chem. Commun*., 2005, 2924–2926; (d) Z. Lin, S. Ou, C. Duan, B. Zhang and Z. Bai, *Chem. Commun*., 2006, 624-626; (e) Z. Lin, Y. Zhao, C. Duan, B. Zhang and Z. Bai, Dalton Trans., 2006, 3678–3684; (f) X.-F. Shang, J. Li, H. Lin, P. Jiang, Z.-S. Cai and H.-K. Lin, *Dalton Trans*., 2009, 2096–2102; (g) T. Kundu, A. D. Chowdhury, D. De, S. M. Mobin, V. G. Puranik, A. Datta and G. K. Lahiri, *Dalton Trans*., 2012, **41**, 4484-4496; (h) D. Amilan Jose, P. Kar, D. Koley, B. Ganguly, W. Thiel, H. N. Ghosh and A. Das, *Inorg. Chem*. 2007, **46**, 5576-5584; (i) S. Li, C. Zhang, S. Huang, F. Hu, J. Yin and S. H. Liu, *RSC Advance*, 2012, **2**, 4215-4219;

9 J.-M. Chen, X.-M. Zhuang, L.-Z. Yang, L. Jiang, X.-L. Feng and T.-B. Lu, *Inorg. Chem*. 2008, **47**, 3158-3165.

10 L. Wang and M. E. Meyerhoff, *Anal. Chim. Acta*., 2008, **611**, 97-102.

11 Y. Li, L. Cao, and H. Tian, *J. Org. Chem*. 2006, **71**, 8279-8282.

12 J.-M. Liu, L. Lin, X.-X. Wang, L. Jiao, M.-L. Cui, S.-L. Jiang, W.-L. Cai, L.-H. Zhang and Z.-Y. Zheng, *Analyst*, 2013, **138**, 278-283.

13 Y. Fan, Y.-M. Zhu, F.-R. Dai, L.-Y. Zhang and Z.-N. Chen, *Dalton Trans.*, 2007, 3885–3892.

14 C. Yang, J. Xu, J. Ma, D. Zhu, Y. Zhang, L. Liang and M. Lu, *Polym. Chem*., 2012, **3**, 2640–2648.

15 (a) B. Zhang, J. Xu, Y. Zhao, C. Duan, X. Cao and Q. Meng, *Dalton Trans*., 2006, 1271–1276; (b) P. D. Beer, *Acc. Chem. Res.* 1998, **31**, 71-80; (c) H. Yamamoto, A. Ori, K. Ueda, C. Dusemund and S. Shinkai, *Chem. Commun*., 1996, 407-408; (d) C. Dusemund, K. R. A. Samankumara Sandanayake and S. Shinkai, *J. Chem. Soc., Chem. Commun*., 1995, 333-334; (e) P. D. Beer and E. J. Hayes, *Coord. Chem. Rev*. 2003, **240**, 167-189; (f) H. Zhang, J. Hu and D.-H. Qu, *Org. Lett*., 2012, **14**, 2334-2337; (g) A. Thakur, D. Mandal, S. Sao, S. Ghosh, *J. Organomet. Chem*., 2012, **715**, 129-135; (h) S. Devaraj, V. S. Elanchezhian, M. Kandaswamy, *Inorg. Chem. Commun*., 2011 **14**, 1596-1601.

16 (a) Y. Chen, Y. Zhou and J. Qu, *Organometallics* 2008, **27**, 666-671; (b) Y. Chen, Y. Zhou, P. Chen, Y. Tao, Y. Li and J. Qu, *J. Am. Chem. Soc.* 2008, **130,** 15250-15251; (c) Y. Chen, L. Liu, Y. Peng, P. Chen, Y. Luo and J. Qu, *J. Am. Chem. Soc.* 2011,

133, 1147-1149; (d) Y. Chen, P. Chen, J. Zhao, L. Liu, Y. Li, S. Chen and J. Qu, *Dalton Trans*. 2010, **39**, 3020-3025; (e) Y. Li, Y. Li, B. Wang, Y. Luo, D. Yang, P. Tong, J. Zhao, L. Luo, Y. Zhou, S. Chen, F. Cheng and J. Qu, *Nat. Chem*. 2013, **5**, 320-326; (f) X. Dong, L. Liu, Y. Zhou, J. Liu, Y. Zhang, Y. Chen and J. Qu, *Dalton Trans.*, 2015, **44**, 14592-14598.

17 (a) J. M. Bollinger, Jr., D. E. Edmondson, B. H. Huynh, J. Filley, J. R. Norton and J. Stubbe, *Science* 1991, **253**, 292-298; (b) A. B. Tomter, G. Zoppellaro, N. H. Andersen, H. P. Hersleth, M. Hammerstad, A. K. Røhr, G. K. Sandvik, K. R. Strand, G. E. Nilsson, C. B. Bell III, A. L. Barra, E. Blasco, L. L. Pape, E. I. Solomon and K. K. Andersson, *Coord. Chem. Rev.* 2013, **257**, 3-26.

18 (a) E. Y. Tshuva, and S. J. Lippard, *Chem. Rev.* 2004, **104**, 987-1012; (b) Q. Fei, M. T. Guarnieri, L. Tao, L. M. L. Laurens, N. Dowe and P. T. Pienkos, *Biotechnol. Adv*. 2014, **32**, 596-614.

19 (a) J. R. Shaffer, J. C. Carlson, B. O. C. Stanley, E. Feingold, M. Cooper, M. M. Vanyukov, B. S. Maher, R. L. Slayton, M. C. Willing, S. E. Reis, D. W. McNeil, R. J. Crout, R. J. Weyant, S. M. Levy, A. R. Vieira and M. L. Marazita, *Hum Genet*. 2015, **134**, 159-167; (b) D. L. Ozsyath, *Rev Environ Sci Biotechnol*. 2009, **8**, 59-79; (c) J. Aaseth, M. Shimshi, J. L. Gabrilove and G. S. Birketvedt, *J. Trace Elem. Med. Bio*. 2004, **17**, 83-92.

20 P. D. Frisch, M. K. Lioyd, J. A. Mccleverty and D. Seddon, *J. Chem.* Soc., *Dalton Trans*. 1973, 2268-2272.

21 A. L. Garner and K. Koid, *J. Am. Chem. Soc*. 2008, **130**, 16472-16473.

22 S. Hua, S. Zhang, C. Gao, C. Xu and Q. Gao, *Spectrochim Acta Part A*: *Molecular and Biomolecular Spectroscopy* 2013, **113**, 325-331.

23 M. Boiocchi, L. D. Boca, D. E. Gómez, L. Fabbrizzi, M. Licchelli and E. Monzani, *J. Am. Chem. Soc.* 2004, **126**, 16507-16514.

24 T. Gunnlaugsson, A. P. Davis, J. E. O'Briena and M. Glynna, *Org. Biomol. Chem*., 2005, **3**, 48-56.

25 J. del Mármol, O. Filevich and R. Etchenique, *Anal. Chem*. 2010, **82**, 6259-6264.

26 J. Y. Kwon, Y. J. Jang, S. K. Kim, K. H. Lee and J. Yoon, *J. Org. Chem*., 2004, **69**, 5155-5157.

27 G. M. Sheldrick, SADABS, *Program for area detector adsorption correction*, Institute for Inorganic Chemistry, University of Göttingen, Germany, 1996.

28 (a) G. M. Sheldrick, *SHELXL-97*, *Program for refinement of crystal structures*, University of Göttingen, Germany, 1997; (b) G. M. Sheldrick, *SHELXS-97*, *Program for solution of crystal structures*, University of Göttingen, Germany, 1997.

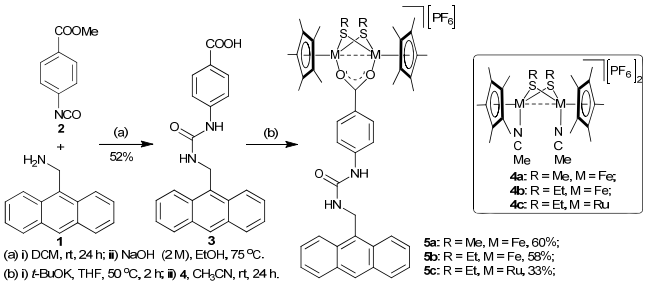

Scheme 1 Synthesis of **5a** - **5c**.

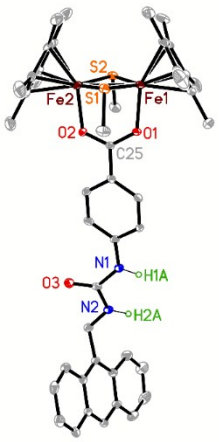

Fig. 1 ORTEP (ellipsoids at 30% probability) diagram of **5a**. The other molecular **5a**, solvent molecular CH_2Cl_2, all hydrogen atoms as well as the PF_6^- anions are omitted for clarity. Selected bond length (Å), Bond Angles and Plane Angles (deg): Fe(1)–Fe(2) 2.5996(10), Fe(1)–S(1) 2.2031(15), Fe(1)–S(2) 2.2115(15), Fe(1)–O(1) 1.972(3), Fe(2)–S(1) 2.2025(16), Fe(2)–S(2) 2.2085(15), Fe(2)–O(2) 1.972(3), Fe(2)–S(1)–Fe(1) 53.83(4), Fe(2)–S(2)–Fe(1) 53.92(4), O(2)–C(25)–O(1) 124.7(4), Cp*(1)-Cp*(2) 55.94(15), S(1)Fe(2)Fe(1)-Fe(2)O(2)O(1)Fe(1) 86.7(7), O(2)C(25)O(1)-Fe(2)O(2)O(1)Fe(1) 4.4(4).

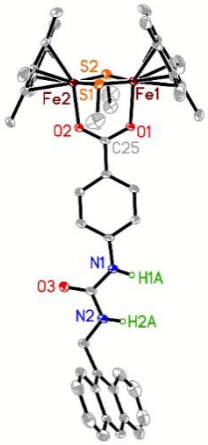

Fig. 2 ORTEP (ellipsoids at 30% probability) diagram of **5b**. All hydrogen atoms as well as the PF_6^- anions are omitted for clarity. Disorder is omitted for clarity. Selected bond length (Å), Bond Angles and Plane Angles (deg): Fe(1)–Fe(2) 2.6208(8), Fe(1)–S(1) 2.2067(13), Fe(1)–S(2) 2.2097(13), Fe(1)–O(1) 1.972(3), Fe(2)–S(1) 2.2008(12), Fe(2)–S(2) 2.1976(12), Fe(2)–O(2) 1.976(3), Fe(2)–S(1)–Fe(1) 53.70(3), Fe(2)–S(2)–Fe(1) 53.59(3), O(2)–C(25)–O(1) 124.8(3), Cp*(1)-Cp*(2) 54.03(12), S(1)Fe(2)Fe(1)-Fe(2)O(2)O(1)Fe(1) 90.0(7), O(2)C(25)O(1)-Fe(2)O(2)O(1)Fe(1) 1.2(4).

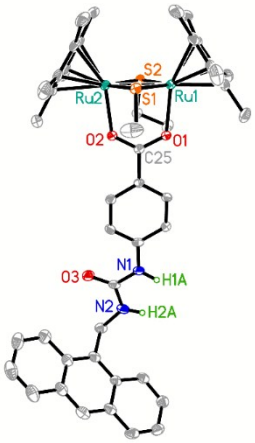

Fig. 3 ORTEP (ellipsoids at 30% probability) diagram of **5c**. All hydrogen atoms as well as the PF_6^- anions are omitted for clarity. Selected bond length (Å), Bond Angles and Plane Angles (deg): Ru(1)–Ru(2) 2.7080(4), Ru(1)–S(1) 2.3045(9), Ru(1)–S(2) 2.3079(8), Ru(1)–O(1) 2.124(2), Ru(2)–S(1) 2.2966(9), Ru(2)–S(2) 2.3156(9), Ru(2)–O(2) 2.108(2), Ru(2)–S(1)–Ru(1) 54.08(2), Ru(2)–S(2)–Ru(1) 54.02(2), O(2)–C(25)–O(1) 125.5(3), Cp*(1)-Cp*(2) 62.9(9), S(1)Ru(2)Ru(1)-Ru(2)O(2)O(1)Ru(1) 89.9(4), O(2)C(25)O(1)-Ru(2)O(2)O(1)Ru(1) 5.9(2).

Table 1. Crystal Data and Structure Refinement for complexes **5a**, **5b** and **5c**.

	5a·1.5 CH_2Cl_2	**5b**	**5c**
Formula	$C_{46.5}H_{56}F_6Cl_3Fe_2N_2O_3PS_2$	$C_{47}H_{57}F_6Fe_2N_2O_3PS_2$	$C_{47}H_{57}F_6N_2Ru_2O_3PS_2$
Formula weigh	1118.07	1018.74	1109.18
Crystal dimensions (mm^3)	0.32×0.16×0.11	0.33×0.21×0.04	0.34×0.16×0.08
Crystal system	Triclinic	Monoclinic	Monoclinic
Space group	*P-1*	$P2_1/c$	$P2_1/c$
a (Å)	13.3872(4)	17.6823(6)	9.5698(3)
b (Å)	17.0602(6)	15.2698(5)	33.4071(11)
c (Å)	22.4013(7)	18.2002(7)	15.0363(5)
α (°)	85.1417(15)	90.00	90.00
β (°)	89.6624(15)	105.609(2)	99.2550(10)
γ (°)	75.2148(15)	90.00	90.00
Volume ($Å^3$)	4928.4(3)	4732.9(3)	4744.5(3)
Z	4	4	4
T (K)	173(2)	173(2)	173(2)
*D*calcd (g cm^{-3})	1.507	1.430	1.553
μ (mm^{-1})	0.934	0.801	0.824
F (000)	2308	2120	2264
No. Of rflns. collected	88123	79966	63927
No. Of indep. Rflns. /Rint	17282 / 0.0960	8327 / 0.0704	8351 / 0.0395
No. Of obsd. Rflns. [$I > 2\sigma(I)$]	11652	6151	7165
Data / restraints / parameters	17282 / 114 / 1185	8327 / 0 / 552	8351 / 0 / 552
R_1, [a] /wR_2 [b] [$I > 2\sigma(I)$]	0.0685 / 0.1623	0.0573 / 0.1425	0.0373 / 0.0856
R_1, [a] /wR_2 [b](all data)	0.1153 / 0.1798	0.0859/ 0.1543	0.0487 / 0.0891
GOF (on F^2)	1.000	1.000	1.000
Largest diff. Peak and hole (e $Å^{-3}$)	1.755 / -1.398	1.734/ -0.711	0.506 / -0.676

[a] $R_1 = \Sigma Fo - |F_c| / \Sigma |F_o|$. [b] $wR_2 = \{\Sigma[w(F_o^2 - F_c^2)^2] / \Sigma[w(F_o^2)^2]\}^{1/2}$.

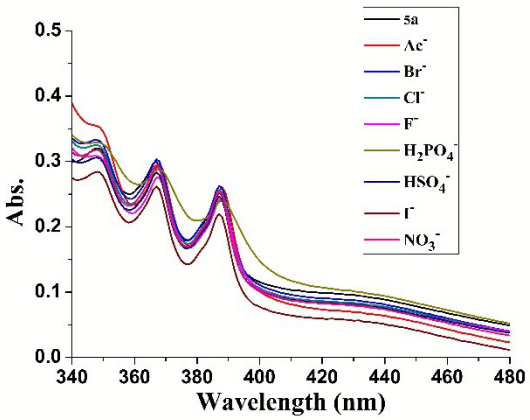

Fig. 4 Absorption spectra of chemosensor **5a** (1×10^{-5} M) upon addition of various anions (3 equiv) in THF solution.

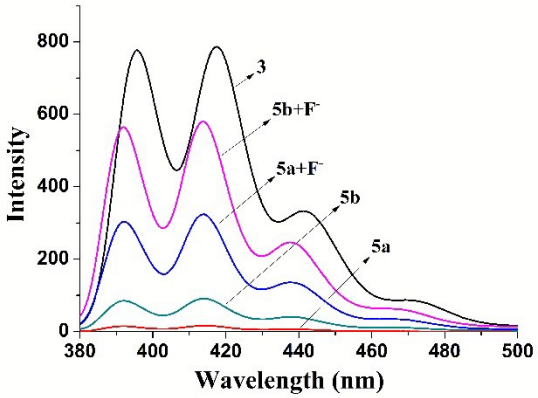

Fig. 5 The fluorescence emission of Ligand **3** (10^{-5} M in DMSO) and **5a** and **5b** (10^{-5} M in THF) before and after upon addition of F^- excited with 370 nm.

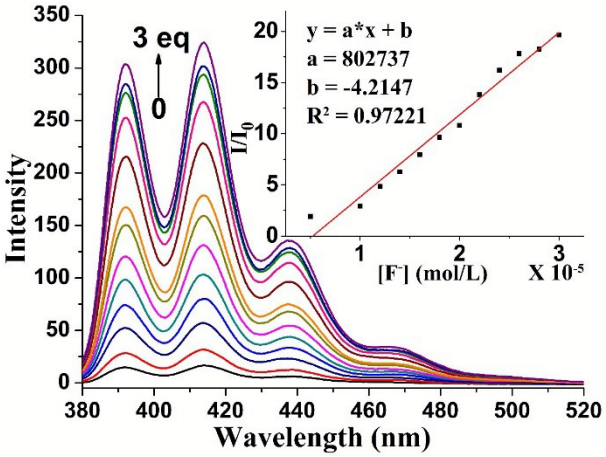

Fig. 6 Fluorescence emission spectra of chemosensor **5a** (10^{-5} M in THF) upon various addition of F^- (as its TBA salt) (0 - 3 equiv). Inset: the ratio of I to I_0 *vs.* the concentration of F^- added. I represents the intensity of **5a** upon addition of F^- and I_0 represents the **5a** original emission intensity at 414 nm excited with 370 nm.

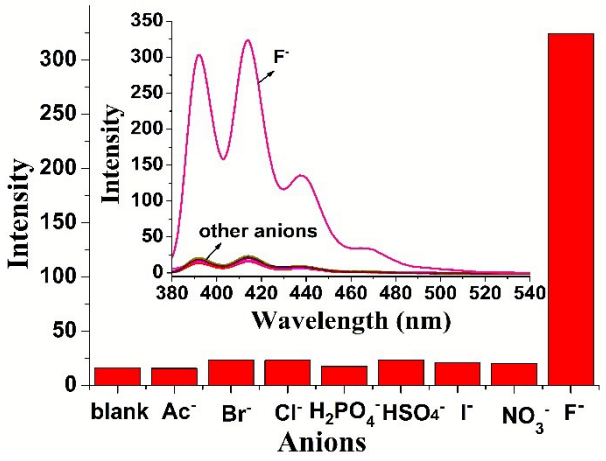

Fig. 7 Selectivity of chemosensor **5a** (10^{-5} M in THF) upon addition of different anions (as their TBA salts) excited with 370 nm.

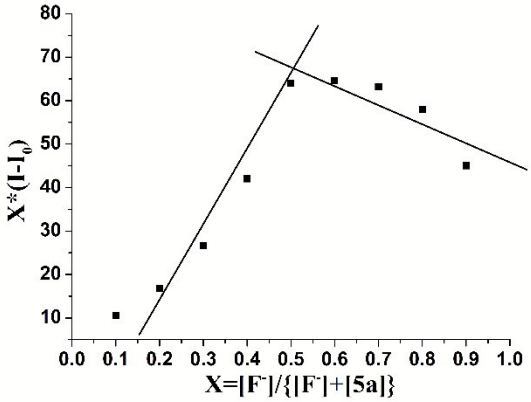

Fig. 8 Job's plot for determining the stoichiometry for chemosensor **5a** and F^- in THF excited with 370 nm. Total concentration of **5a** + Fe^{3+} = 2.5×10^{-5} M. I represents the intensity of **5a** upon addition of F^- and I_0 represents the **5a** original emission intensity at 414 nm excited with 370 nm.

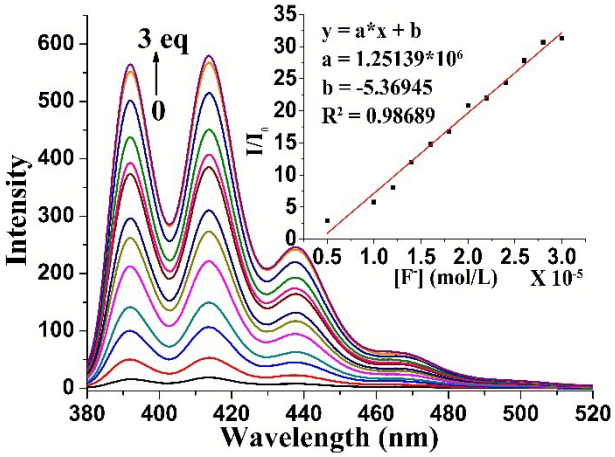

Fig. 9 Fluorescence emission spectra of chemosensor **5b** (10^{-5} M in THF) upon various addition of F^- (as its TBA salt) (0 - 3 equiv). Inset: the ratio of *I* to I_0 *vs.* the concentration of F^- added. *I* represents the intensity of **5b** upon addition of F^- and I_0 represents the **5b** original emission intensity at 414 nm excited with 370 nm.

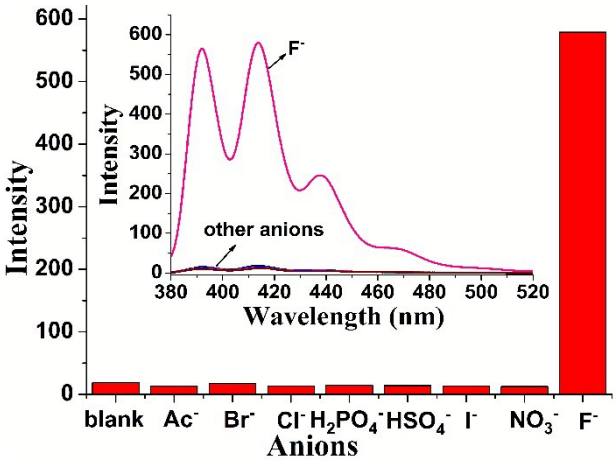

Fig. 10 Selectivity of chemosensor **5b** (10^{-5} M in THF) upon addition of different anions (as their TBA salts) excited with 370 nm.

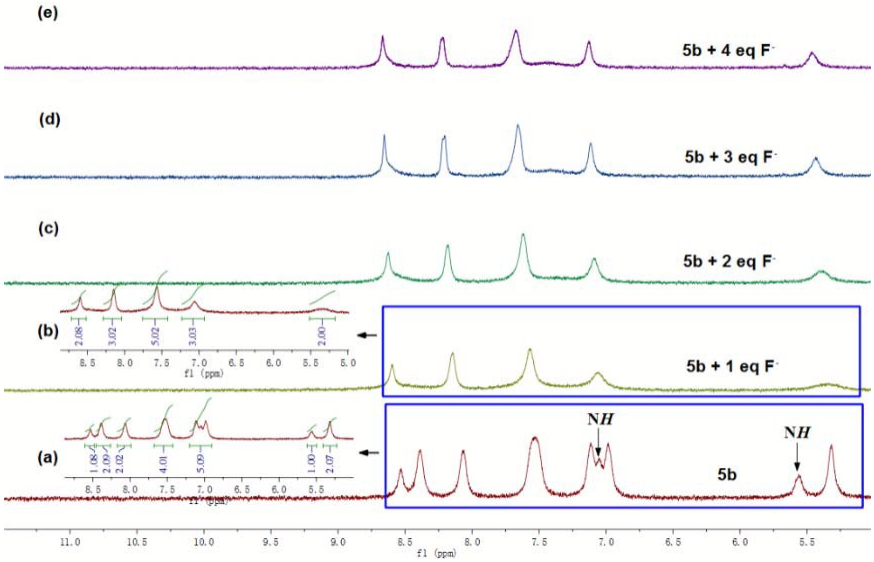

Fig. 11 The changes of ^{1}H NMR (CD_3CN, 400 MHz) spectra for **5b** upon addition of different equivalents of F^-

For Table of Contents Only

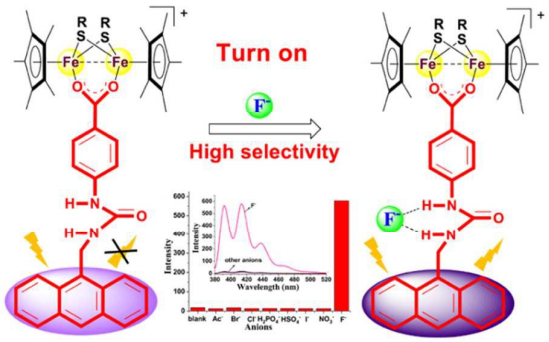

The diiron-sulfur clusters bearing urea and anthracene units showed rapid and selective recognition for fluoride ion.